Chemical Engineering Journal 387 (2020) 124072

Contents lists available at ScienceDirect

Chemical Engineering Journal

journal homepage: www.elsevier.com/locate/cej

Applying machine learning algorithms in estimating the performance of heterogeneous, multi-component materials as oxygen carriers for chemical-looping processes

Yongliang Yan[a,b], Tobias Mattisson[b], Patrick Moldenhauer[b], Edward J. Anthony[a], Peter T. Clough[a,*]

[a] Energy and Power Theme, School of Water, Energy and Environment, Cranfield University, Cranfield, Bedfordshire MK43 0AL, UK
[b] Division of Energy Technology, Department of Space, Earth and Environment, Chalmers University of Technology, 412 96 Gothenburg, Sweden

HIGHLIGHTS

- Machine learning is used to estimate the performance of oxygen carriers for chemical-looping.
- The workflow for applying machine learning in oxygen carriers is elucidated.
- Artificial neural networks are used to predict the reactivity of manganese ores.
- Bootstrap resampling is used to add the confidence intervals to the predicted data.
- A high prediction accuracy was achieved when testing these models on unseen data.

GRAPHICAL ABSTRACT

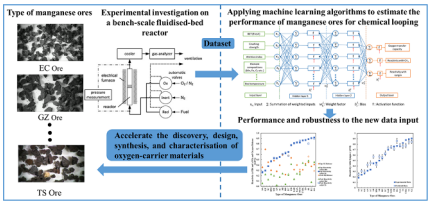

ARTICLE INFO

Keywords:
Machine learning
Artificial neural network
Manganese ores
Oxygen-carrier materials
Chemical-looping

ABSTRACT

Heterogeneous, multi-component materials such as industrial tailings or by-products, along with naturally occurring materials, such as ores, have been intensively investigated as candidate oxygen carriers for chemical-looping processes. However, these materials have highly variable compositions, and this strongly influences their chemical-looping performance. Here, using machine learning techniques, we estimate the performance of heterogeneous, multi-component materials as oxygen carriers for chemical-looping. Experimental data for 19 manganese ores chosen as potential chemical-looping oxygen carriers were used to create a so-called training database. This database has been used to train several supervised artificial neural network models (ANN), which were used to predict the reactivity of the oxygen carriers with different fuels and the oxygen transfer capacity with only the knowledge of reactor bed temperature, elemental composition, and mechanical properties of the manganese ores. This novel approach explores ways of dealing with the training dataset, learning algorithms and topology of ANN models to achieve enhanced prediction precision. Stacked neural networks with a bootstrap resampling technique have been applied to achieve high precision and robustness on new input data, and the confidence intervals were used to assess the precision of these predictions. The current results indicate that the best trained ANNs can produce highly accurate predictions for both the training database and the unseen data with the high coefficient of determination (R^2 = 0.94) and low mean absolute error (MAE = 0.057). We envision that the application of these ANNs and other machine learning algorithms will accelerate the development

* Corresponding author.
E-mail address: P.T.Clough@cranfield.ac.uk (P.T. Clough).

https://doi.org/10.1016/j.cej.2020.124072
Received 18 September 2019; Received in revised form 4 January 2020; Accepted 8 January 2020
Available online 09 January 2020

of oxygen carrying materials for a range of chemical-looping applications and offer a rapid screening tool for new potential oxygen carriers.

1. Introduction

Chemical-looping combustion (CLC) and chemical-looping with oxygen uncoupling (CLOU) are state-of-the-art methods for heat and power production, which can achieve CO_2 separation at low cost and with very low energy penalties [1]. The chemical-looping process is carried out in a dual fluidised-bed reactor system, where the oxygen is transported from an air reactor to a fuel reactor by means of an oxygen carrier [2]. The chemical-looping concept can also be integrated with steam reforming (SR-CLC) for H_2 production or operated under partial oxidation for chemical-looping gasification (CLG) and reforming (CLR) to generate a syngas [3–7]. Furthermore, CLC can be implemented in current fluidised bed boilers through oxygen-carrier-aided combustion (OCAC), which partially or completely replaces bed materials with oxygen-carrier materials to enhance the combustion process [8,9].

In CLC, the fuel, here idealised as a pure hydrocarbon (C_nH_{2m}), is oxidised by the oxygen carrier, here denoted as a metal oxide (M_yO_x) to produce CO_2 and steam [1,10] according to the following global reaction scheme:

$$(2n + m)M_yO_x + C_nH_{2m} \rightarrow (2n + m)M_yO_{x-1} + mH_2O + nCO_2 \quad (1)$$

Subsequently, the reduced oxygen carrier particles are reoxidised by air as shown in Reaction (2).

$$M_yO_{x-1} + \frac{1}{2}O_2 \rightarrow M_yO_x \quad (2)$$

For CLOU, gaseous oxygen is released from the oxygen carrier, Reaction (3), and thereafter, the fuel reacts with the gas-phase oxygen as in normal combustion processes to produce CO_2 and H_2O through Reaction (4), allowing easy separation of CO_2 by condensing the steam. The reduced oxygen carrier is regenerated by Reaction (2) in the air reactor [1].

$$M_yO_x \rightarrow M_yO_{x-1} + \frac{1}{2}O_2 \quad (3)$$

$$\left(n + \frac{1}{2}m\right)O_2 + C_nH_{2m} \rightarrow mH_2O + nCO_2 \quad (4)$$

Over the last two decades, extensive research has been conducted on the chemical-looping process focused on reactor design, oxygen-carrier materials development and continuous operation testing [11]. Currently, the overall technology readiness level (TRL) for CLC is estimated as TRL 6, and well over a 1000 materials based on Ni, Cu, Fe, Mn, Co, as well as other mixed oxides and inexpensive materials, have been investigated at different research institutes, e.g., ICB-CSIC in Zaragoza, Vienna University of Technology, Technical University Darmstadt, Ohio State University, University of Utah, Southeast University in Nanjing, and Chalmers University of Technology in Gothenburg among others [3,12,13]. In addition, a range of materials have been successfully tested in long-term, continuous operation in CLC facilities from 0.3 kW_{th} to 1 MW_{th} worldwide [11,14].

A key barrier to chemical-looping technologies development is the selection of the optimal oxygen-carrier materials according to the criteria of cost, availability, reactivity, oxygen transfer capacity as well as stability over a large number of reduction/oxidation cycles [3,15,16]. Many reviews are available, which provide a detailed summary of experience and knowledge related to CLC oxygen carrying [3,10,14,16–18].

Besides the investigation of pure and synthetic metal oxides for oxygen carrying materials, ores and industrial products as oxygen carriers have attracted great interest due to their low cost and availability, especially where they offer sufficient reactivity for use with solid fuels. Leion et al. [19,20] conducted a series of tests to identify suitable candidates as oxygen carrying materials for CLC based on Fe- and Mn-containing ores as well as industrial products in a bench-scale, batch fluidised bed reactor. Later on, researchers studied the feasibility of using Norwegian industrial tailings as well as minerals and ores as the oxygen carrying materials for CLC. The results indicated that manganese ores represent a promising candidate for use in CLC processes [15]. The high reactivity seen with Mn-based materials may be explained by the propensity of such materials to release oxygen to the gas phase, or having CLOU properties. Arjmand et al. [21] evaluated six different manganese ores as oxygen carrier for CLC of solid fuels. Sundqvist et al. [22,23] invested the reactivity of 19 different manganese ores with methane and syngas, as well as their oxygen uncoupling behaviour in a batch, fluidised-bed reactor. The results indicated that some of these manganese ores exhibited high reactivity with different gaseous fuels, had lower attrition rates and low cost; and in summary, they were promising candidates for CLC processes. In addition, many ores and industrial products, such as iron ores, ilmenite, manganese ores and slags, have been tested in continuous CLC operation processes and show promising behaviour [24–31].

Unfortunately, such ores and industrial products have highly variable compositions, and contain heterogeneous, multi-component phases and, hence, their performance may vary significantly. For Mn ores, this may be particularly true, as it is well known that common impurities affect the thermodynamics to a large extent. Therefore, some researchers have suggested that extensive investigation on heterogeneous, multi-component materials may be necessary to determine if they are suitable for chemical-looping [19].

Given the versatility of Artificial Intelligence (AI), various areas, such as games, automation, medical and process control, have begun to apply AI to achieve improved performance, prediction of unmeasured parameters, or pattern recognition [32]. Machine learning (ML), which can be classified into supervised, unsupervised and reinforcement learning, is part of the wider spectrum of AI technology that applies statistical techniques to allow models to progressively improve performance [33]. Artificial neural networks (ANNs) are one of the most widely applied machine learning approaches. Inspired by the learning behaviour of the human brain, ANNs have been widely applied in various applications, including control, robotics, pattern recognition, forecasting, medicine, power systems, manufacturing, optimisation, signal processing, and social/psychological science [34,35]. ANNs can act as a “black box” that can generate the desired output given a set of input data, and they can learn from the historical data and are able to deal with different disciplines for tasks such as prediction, classification, and pattern recognition [36,37].

Recently, ANN has been used in carbon capture technologies, mainly focused on the process modelling and control of amine-based post-combustion technology [38–41]. In terms of carbon capture materials, some researchers proposed using large-scale computational screening to aid the experimental investigation to discover novel materials for calcium looping and chemical-looping [42,43]. However, to the best of our knowledge, ANNs or other machine learning algorithms have not been applied to the area of oxygen carriers for chemical-looping processes. To develop the next generation of chemical-looping materials and reduce the time and cost of material development, it is necessary to evaluate whether data-driven ML algorithms can allow us to exploit valuable information contained in historical experimental data to assist the design and manufacture of optimal oxygen carriers. Further, for complex natural oxygen carriers, the multi-element, multi-

phase environment makes it very difficult to predict behaviour using traditional chemical characterisation, and here data-driven approaches could be of significant use for determining important parameters, and provide guidance for what to search for in natural systems.

In this work, we explore the potential application of ML algorithms in estimating the performance of heterogeneous, multi-component materials as oxygen carriers for chemical-looping processes. Feedforward backpropagation artificial neural networks that can predict the reactivity of manganese ores as oxygen carriers for CLC/CLOU are used as an example to illustrate the feasibility of applying ML in the development of oxygen-carrier materials. The experimental data of different manganese ores in CLC/CLOU under a bench-scale, batch fluidised-bed reactor have been used as the datasets to develop the ANN models, and then the performance of the trained ANN for estimation of the reactivity of manganese ores as oxygen carriers has been discussed.

2. Methodology

2.1. Materials

In this work, 19 manganese ores from various suppliers around the world were analysed. These ores were first calcined in air at 950 °C for 24 h in a box furnace, and then crushed and sieved to a particle size fraction of 125–180 μm. Their elemental compositions were analysed and determined by ICP-SFMS (Inductively-Coupled Plasma – Sector Field Mass Spectrometry). The results of elemental compositions and physical properties such as attrition index, crushing strength and BET surface area are shown in Table 1. It is clear that the ores contain a significant fraction of metals and semi-metals in addition to manganese. For instance, enhanced levels of Fe, Si, Ca and Mg, all components which can affect CLC behaviour, are present.

2.2. Experimental investigation

The experimental investigations with the manganese ores were conducted in a batch fluidised-bed reactor. A quartz liner (820 mm long, 22 mm I.D.) was placed inside the main body of the reactor and a porous quartz plate, the gas distributor, was located 370 mm from the bottom. The reactor was heated with an electrical furnace and the fluidisation of particles was monitored by the pressure fluctuations over the reactor. Gases controlled by mass flow controllers were injected from the bottom of the reactor to enable fluidisation of the particles. From the outlet of the reactor, the exhaust gases were sent to a cooler to remove the moisture from the gas stream. Subsequently, the volumetric flow and gas composition of the dry gas stream were analysed with a Rosemount NGA 2000 multi-component gas analyser, where concentrations of CH_4, CO, CO_2 and O_2 were measured.

The performance of the manganese ores was assessed with regard to their oxygen release and reactivity towards methane and syngas (50% CO in H_2) at three temperatures (900 °C, 950 °C and 1000 °C). Additional tests for their performance with syngas were conducted at bed temperature of 850 °C. The CO_2 yield from syngas and methane conversion are given in Eqs. (5) and (6), respectively. A schematic description of the experimental system and more details of the experimental investigation can be found elsewhere [22,23,44]

$$\gamma_{CO} = \frac{P_{CO_2}}{P_{CO} + P_{CO_2}} \tag{5}$$

$$\gamma_{CH_4} = \frac{P_{CO_2}}{P_{CO} + P_{CO_2} + P_{CH_4}} \tag{6}$$

2.3. Estimation of reactivity of manganese ores using the artificial neural network

2.3.1. Background of artificial neural network

Artificial neural networks are composed of input, hidden and output layers as well as a number of parallel-interconnected neurons in each layer. The input data are received by the neurons of the input layer and the output of each input neuron feeds into the neurons of a hidden layer. Then their output is transferred either through more hidden layers or directly to the output layer to achieve the results or predictions. With the tuning of activation functions by adjusting the weight and bias vectors between the neurons in each layer, the prediction performance can be enhanced. The above process of single-layer networks can be expressed by the following equation:

$$y_n = f\left(\sum_{i=1}^{n} x_n w_i^n + b_i^n\right) \tag{7}$$

Herein, y_n are the output signals of the current layer and input signals of neurons of the next layer; x_n are the input signals of the network; w_i^n and b_i^n are the values of weights and biases between the neurons, respectively. f is the activation function, where a sigmoid function is usually applied, as shown in Eq. (8).

$$f_{(x)} = \frac{1}{1 + e^{-x}} \tag{8}$$

The training process of the ANNs aims to achieve the lowest root mean square error (RMSE) and mean absolute error (MAE) (described by Eqs. (9) and (10)) and the highest coefficient of determination (R^2)

Table 1
Elemental compositions and physical properties of the manganese ores investigated.

Composition (wt%) and properties	EB	EC	AN	AC	SB	SA	GZ	SC	BR	EG	GL	MT	NCH	SL	SAB	SAA	UMK	TS	HM
Mn	32.42	11.53	35.31	34.59	54.76	52.60	18.01	46.11	58.36	50.44	34.59	15.85	42.51	36.75	46.83	38.91	61.97	42.51	53.32
Fe	21.70	51.80	11.90	10.50	16.10	9.10	28.70	5.18	3.57	10.50	5.88	35.70	11.90	4.13	11.90	16.10	3.85	5.39	7.00
Si	4.67	4.57	7.00	6.53	3.17	3.92	7.47	3.73	0.93	0.89	2.85	6.07	1.59	3.03	2.15	1.73	0.93	4.43	1.73
Al	1.22	1.27	1.64	1.69	0.17	2.49	7.41	3.39	1.91	0.32	0.12	1.64	0.22	0.19	0.19	0.26	2.06	0.20	4.55
Ti	0.08	0.07	0.08	0.08	0.01	0.12	0.72	0.23	0.11	0.02	0.01	0.06	0.03	0.01	0.02	0.01	0.10	0.02	0.14
Ca	1.71	0.86	9.29	12.86	2.43	0.93	0.20	1.86	0.14	1.43	8.57	0.59	6.21	8.57	5.93	3.93	0.17	10.71	0.07
K	0.46	0.27	0.21	0.32	0.07	1.08	0.24	1.00	0.61	0.12	0.07	0.34	0.07	0.33	0.07	0.07	0.59	0.17	1.08
Mg	0.84	0.39	3.96	3.54	0.37	0.22	0.56	0.25	0.34	0.96	2.22	0.11	0.60	1.80	0.72	0.41	0.34	2.34	0.07
Na	0.38	0.30	0.07	0.07	0.04	0.21	0.04	0.05	0.04	0.38	0.04	0.04	0.04	0.15	0.04	0.14	0.04	0.08	0.04
P	0.13	0.10	0.06	0.06	0.03	0.10	0.10	0.10	0.06	0.06	0.02	0.04	0.04	0.02	0.04	0.04	0.06	0.02	0.13
Attrition (wt%/h)	3.59	4.07	1.99	4.51	1.29	1.21	2.88	1.37	2.80	4.60	4.30	6.10	2.40	4.30	2.40	2.20	4.90	3.20	8.40
Crushing strength (N)	1.90	1.70	2.80	2.20	3.20	3.40	2.40	3.20	1.90	3.70	4.50	1.80	3.80	3.70	4.70	4.30	4.20	2.60	2.00
BET (m^2/g)	16.40	0.39	0.14	0.61	0.28	0.11	1.46	0.10	1.20	0.75	1.10	1.20	0.86	6.10	0.41	1.20	12.00	0.70	1.40

EB = Elwaleed Grade B, EC = Elwaleed Grade C, AN = Autlan Nodules, AC = Autlan Carbonate, SB = Sibelco Braunite, SA = SinAus, GZ = Guizhou, SC = Sibelco Calcined, BR = Brazilian (Buritirama), EG = Egyptian, GL = Gloria, MT = Metmin, NCH = Nchwaning, SL = Slovakian, SAB = South Africa B, SAA = South Africa A, UMK = United Manganese of Kalahari, TS = Tshipi, HM = Eramet HM.

between the target output (t_i) and predicted output (y_i) from the ANNs by adjusting the weights and biases according to the training algorithms.

$$RMSE = \sqrt{\frac{1}{n}\left[\sum_{i=1}^{n}(t_i - y_i)^2\right]} \quad (9)$$

$$MAE = \frac{1}{n}\left[\sum_{i=1}^{n}|t_i - y_i|\right] \quad (10)$$

The ability of the ANN model to learn and generalise the relationship of practical and complex non-linear processes has developed as a powerful tool to predict the properties and performance in material science [45–51]. The application of ANNs in estimation of the performance of heterogeneous, multi-component materials as oxygen carriers for chemical-looping process ought to provide a cost-effective approach to predict the performance and aid the design of oxygen carriers for chemical-looping. In this work, we consider the general workflow in developing a machine learning model to predict the performance of the oxygen carriers and the potential method to aid the design of the oxygen-carrying materials, as illustrated in Fig. 1. In the following sections, we will illustrate how to reutilise the ANN model trained by the experimental data to predict the reactivity of manganese ores as oxygen carrying materials in CLC/CLOU.

2.3.2. Database

A database that consists of the physical and chemical properties, experimental conditions, reactivity with fuels and oxygen release rates has been established based on previous work [22,23]. From here, one must decide the input and output parameters of the ANNs, and generate the training database from the experimental data. As mentioned earlier, it is well established for manganese ores that the oxygen release behaviour and reactivity with fuels are dependent on the type of the ore, and their properties including elemental compositions, attrition rate, crushing strength and surface area, and experimental investigation conditions (temperature, pressure, flow rate and fuel type). Therefore, fourteen parameters, including the mass concentration of the elements Mn, Fe, Si, Al, Ti, Ca, K, Mg, Na and P, bed temperature, attrition index, crushing strength and BET surface area of the fresh materials, have been considered as inputs of the training database. For the output parameters, the reactivity with syngas, methane and the oxygen release to the gas phase were selected, as they are the most valuable parameters to evaluate the performance and determine whether they are suitable for chemical-looping.

A linear correlation analysis and feature selection by neighbourhood component analysis for regression was performed to select the most important inputs (termed 'feature') out of the 14 possible inputs by calculating the absolute values of Pearson Correlation Coefficients (PCC) (this data is available in the Fig. S.1. to S.3. in the Supplementary Materials) and feature weights (Fig. S.4. in the Supplementary Materials). In this case, the PCC value of 0.5–1 implies a strong linear correlation, whereas 0 indicates a weak linear correlation. For the feature weights analysis, an unimportant input would have a feature weighting close to zero. Based on these analyses, we selected seven out of the initially considered 14 inputs for the reactivity predictions and four out of 14 inputs for oxygen release rate predictions. The seven inputs chosen were bed temperature, crushing strength, and elemental compositions of Al, Ti, P, Si, and K. It is interesting to note that the reactivity with syngas and methane was not found to be highly correlated with the main constituent parts of the ores – Mn and Fe. The four chosen inputs for oxygen releasing rate predictor were bed temperature, and elemental compositions of Fe, Mn, and Si. These reduced input models were compared against ANN models that utilised all 14 inputs, which were able to predict the oxygen release rate and reactivity simultaneously.

The abbreviations of each of the ores investigated are summarised in Table S.1 of the Supplementary Materials. In addition, the experimental data of the reactivity with syngas of 19 different ores at bed temperature 850 °C were selected as an unseen dataset, which was not included in the original training database and only used to assess the performance and robustness of the trained ANNs.

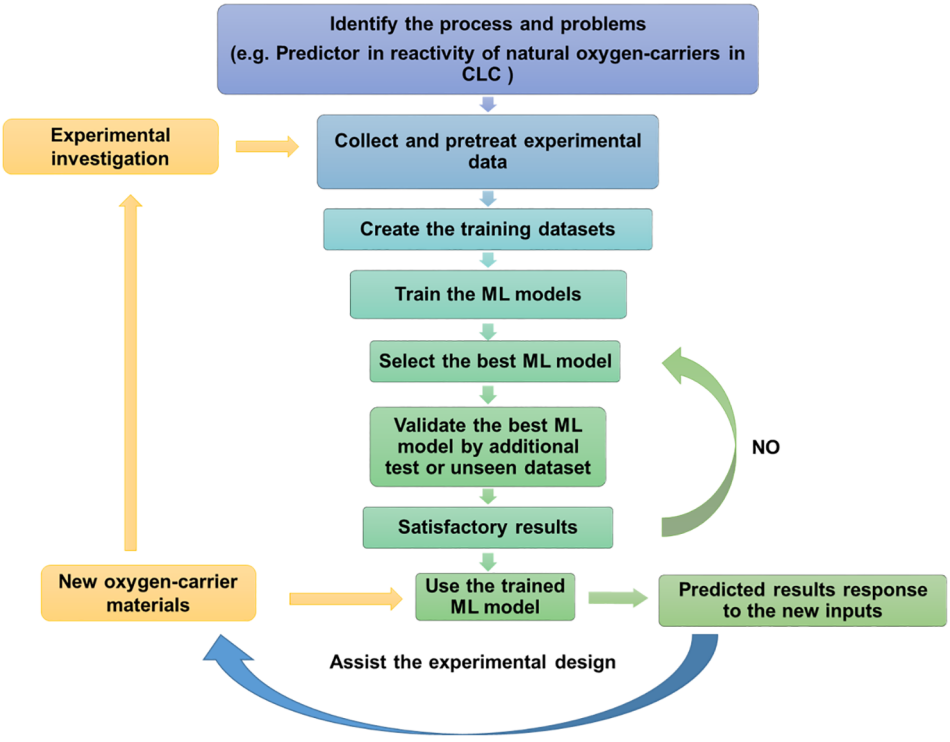

Fig. 1. Workflow of developing a machine-learning model for oxygen carriers in the chemical-looping process.

2.3.3. Optimising artificial neural network models

Once the original training database (171 input-output pairs) was established, the next step was to design and train the ANN models. In this work, MATLAB was used to develop the feedforward ANN models. Three training functions designated as *trainlm, trainbr* and *trainbfg* have been selected to train the multi-layer neural networks. *Trainlm* is a popular fast backpropagation algorithm that updates the weight and bias values according to Levenberg-Marquardt optimisation in supervised learning ANNs. *Trainbr* is the Bayesian regularisation backpropagation algorithm, which minimises a combination of squared errors and weights, and then decides the correct combination to achieve a more generalised neural network. *Trainbfg* is the Broyden–Fletcher–Goldfarb–Shanno (BFGS) quasi-Newton backpropagation algorithm that updates weights and biases according to the BFGS quasi-Newton method. To improve the ANNs generalisation and avoid overfitting, the original training database is randomly divided into different datasets and an "early stopping" mechanism has been applied in the training algorithms. For the *trainlm* and *trainbfg* algorithms, the input data was randomly dived in a training set (70%), validation set (15%) and test set (15%). For the the *trainbr* algorithm, 80% of the dataset was used for training and 20% assigned to the test set for ANNs. No validation set was used for the *trainbr* algorithm because *trainbr* has its own form of validation built into the algorithm. It is also worth noting that the input data of the training database was normalised to values between 0 and 1, before training the ANNs, to prevent any unintended bias occurring in the training data.

It is a complex task to decide the topology (number of neurons and hidden layers) of the ANN and to train the ANN. In order to achieve the optimal ANN model to predict the reactivity of manganese ores, several MATLAB scripts were developed to decide the topology of the ANN. The performances of the ANNs were evaluated by the minimum value of the mean absolute error (MAE) and the highest value of the coefficient of determination (R^2). Single and double hidden layer ANNs were investigated. The single hidden layer ANNs with the number of neurons from one to twenty-five, and two hidden layers ANNs (number of neurons: first hidden layer from one to twenty-five, and second hidden layer from one to thirty-five) were trained and validated with the three training functions. The random number seed was reset at the beginning of each new number of hidden neuron trials. The trained ANNs are then further assessed by the unseen dataset to investigate their performance and robustness to new inputs. The architecture of ANN with two hidden layers is shown in Fig. 2.

3. Results and discussion

3.1. Performance of the trained neural networks

The prediction performance of the trained neural networks was evaluated by the root mean square error (RMSE), the mean absolute error (MAE) and the coefficient of determination (R^2). Lower values of RMSE and MAE, along with higher values of R^2 indicated better-fitting ANN models. The proposed ANN structures with different training algorithms were trained by the original training database. The performances of proposed ANNs were varied with the number of neurons in each hidden layer as shown in Figs S.5. and S.6. Only the single hidden layer neural networks with *trainbr* indicated that the MAE of the ANN decreased when increasing the number of neurons. This is because *trainbr* not only checks the performance of the model, but also determines how large the weights are, and this results in this training method producing more generalised ANN models. Therefore, it is necessary to try different structures of ANNs to optimise the ANN models. Once optimised ANN models were obtained with different hidden layers and number of neurons, the results showed that the data predicted by the ANN models fitted the experimental results well. The performance of the trained neural networks with different topologies and training functions are shown in Table S.2. (14-inputs) and Table S.3. (7-inputs) in the Supplementary materials. The performance of the trained neural networks with the functions *trainlm* and *trainbfg* increased with increasing number of hidden layers, whereas performance with the function *trainbr* was not improved by increasing the number of hidden layers. Furthermore, the reduced input models did not improve the performance of trained ANNs, this is likely due to the strong correlating features not being able to represent all the information within the experimental training data. By only utilising the strongest correlating features, the weak correlating features are excluded and their minor, but important, impact on the final predictions is lost. The authors also suggest that these weaker correlating features are an important part of the dataset that enable the production of a generalised model. Fig. 3 presents a comparison of experimental and predicted data by *trainlm* with different optimised numbers of neurons in the hidden layers at a bed temperature of 900 °C with different numbers of inputs. Further comparisons of the ANN predicted data with the experimental results is presented in Figs. S.7.–S.10. in the Supplementary Materials.

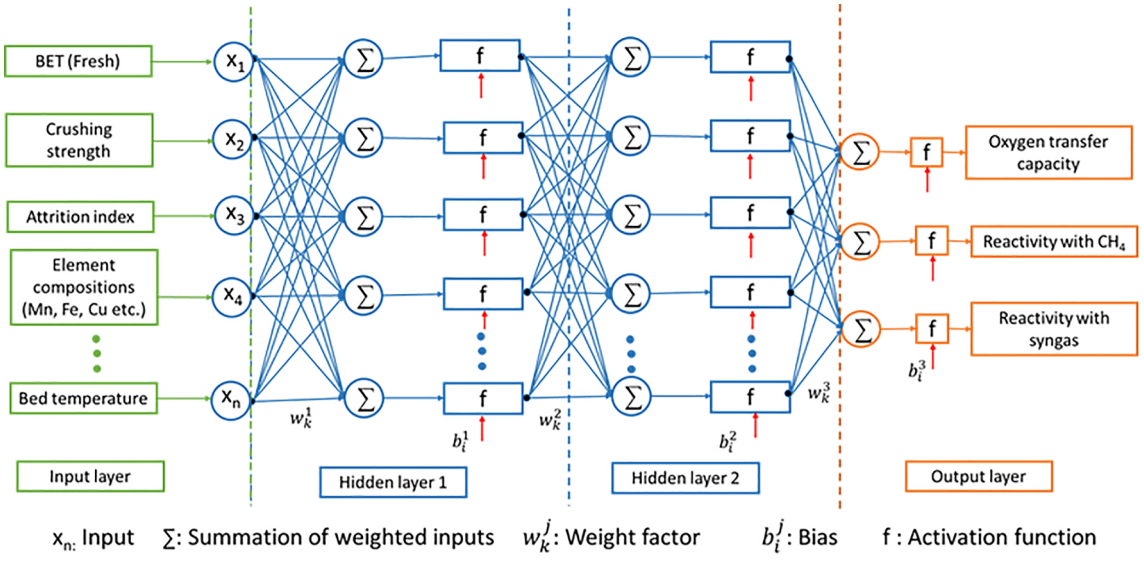

Fig. 2. Proposed neural networks structure to predict the reactivity of manganese ores in the chemical-looping process.

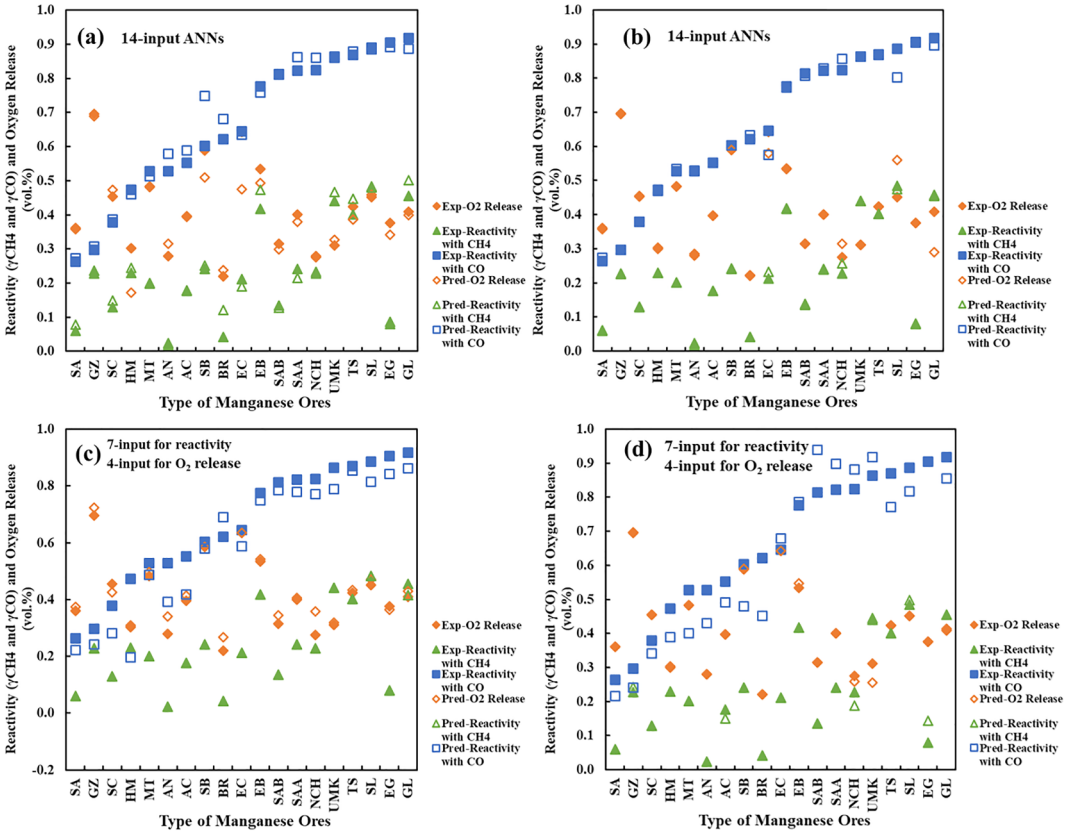

Fig. 3. Experimental and predicted reactivity and oxygen release of manganese ores as oxygen carriers at bed temperature 900 °C- (a) *trainlm* single hidden-layer (14-input ANNs) and (b) *trainlm* two hidden-layer (14-input ANNs) (c) *trainlm* single hidden-layer (7 and 4-input ANNs) (d) *trainlm* two hidden-layer (7 and 4-input ANNs).

3.2. Confirmation of model robustness using unseen data

Another important requirement for the ANN models is that they should not only accurately predict data within the training, validation and testing database but also provide a high prediction accuracy and robustness with new data that was not included within the training database. As previously mentioned, the selected ANNs were utilised to predict the reactivity of manganese ores with syngas at a bed temperature of 850 °C, which formed an unseen dataset to confirm the robustness and generality of the optimised ANNs. In addition, the performance of single optimised ANNs was compared with the stacked ANNs, which combine the results of 50 different ANNs with the same structure and different initial weights and biases. In the case of the performance on the unseen data, the stacked ANNs increased the prediction accuracy significantly over that of the single ANNs. The single hidden layer stacked ANNs trained with *trainbr* achieved the closest match with the experimental data on both the training database and unseen data. Nevertheless, the increase of the number of hidden layers for the stacked ANNs reduces the prediction accuracy on unseen data.

When applying the trained ANNs to predict the results of unseen data, it is necessary to give a confidence interval for the prediction, since closely agreeing results do not automatically mean high precision of the predictions. It can be concluded that based on the data presented in the two-hidden-layer ANNs trained with *trainbr* (14–5-21–3) had the second best performance on the training database, but its stacked ANNs had the worst performance on unseen data, likely caused by overfitting of the ANNs. The network has memorised the relationship of the training dataset, but it has not learned to generalise under new situations. In this work, the bootstrap resampling technique was used to calculate the confidence intervals of predictions of stacked ANNs on unseen data through the function *bootci* in MATLAB, which computes the 95% bootstrap confidence interval based on the estimated standard error of predictions. This is presented as error bars in Figs. 6–8, which show the top three stacked ANNs on reactivity predictions of unseen data with the 95% confidence intervals. In general, the predictions of these three ANNs on unseen data are in good agreement with the experimental data, although there were some discrepancies in the AC, AN and BR manganese ores. This may arise from the fact that most highly correlated input features (identified in the reduced order models) were similar in value but different experimental results were found. There may have been experimental or analytical inaccuracies, or some other material property not captured in the training dataset that could identify the cause of this discrepancy. The average difference between the experimental data and predictions of these three stacked ANNs on the unseen data was 14.7% in Fig. 4(a), 15.2% in Fig. 4(b) and 18.0% in Fig. 4(c). Compared with the reduced order 7-input ANNs (MAE = 0.064 and R^2 = 0.92, Fig. S.11. in the Supplementary Materials), the 14-input ANNs (MAE = 0.057 and R^2 = 0.94) presented a much higher accuracy and robustness to the unseen data.

3.3. Sensitivity analysis

Besides using the trained ANNs to predict the reactivity of manganese ores with different fuels, they can also be used to estimate the potential effect of changing input values on the expected outputs, i.e. a predictive sensitivity analysis. We have selected four input parameters: Fe content, Mn content, BET surface area, and attrition index. Using the average value of each input parameter of all the ores as a baseline, a new dataset was created by varying these parameters by up to ± 50% relative to the normalised inputs. The highest performing stacked ANN model (14-13-3 with *trainbr*) was used to undertake the sensitivity analysis, data from which is shown as Fig. 5. The results from the ANN

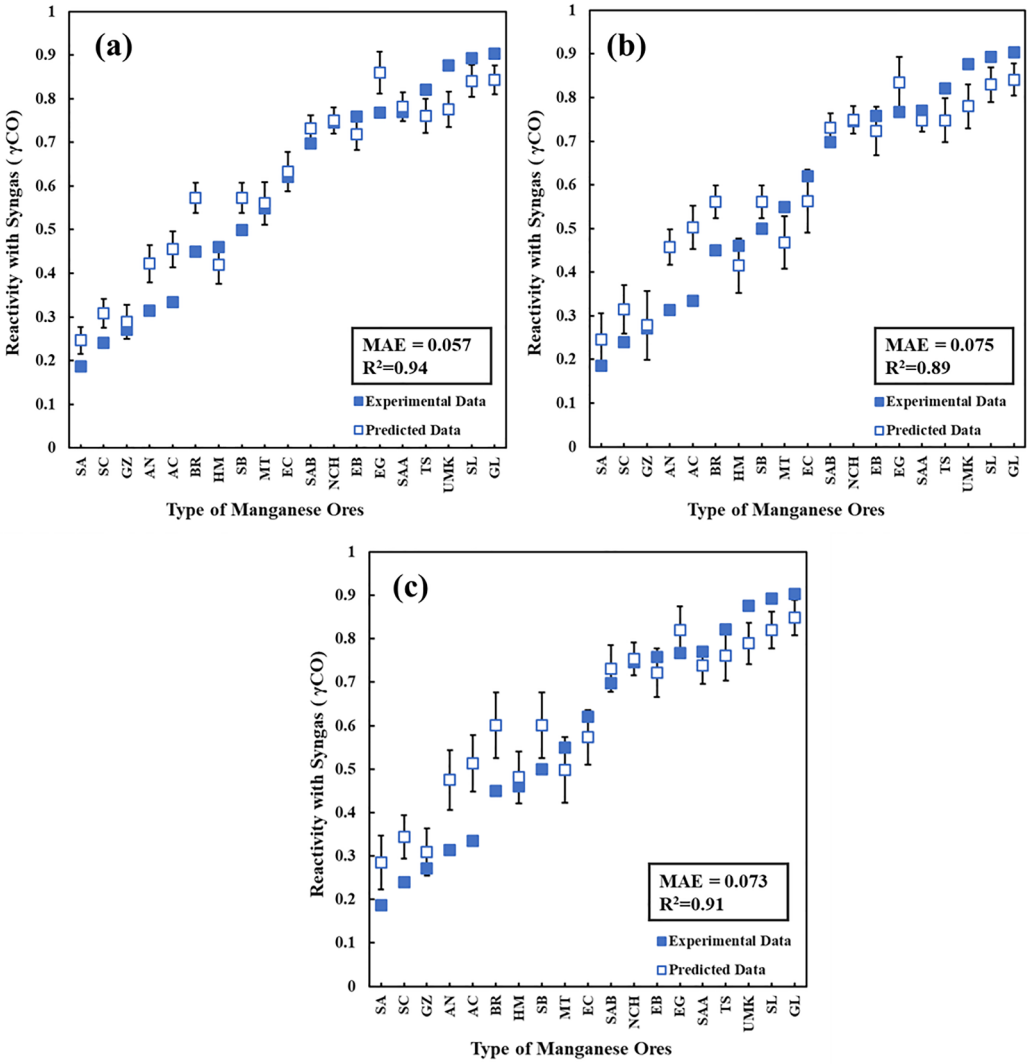

Fig. 4. (a) Predictions of stacked neural network (14-13-3) trained with *trainbr* with 95% confidence intervals on unseen data; (b) Predictions of stacked neural network (14-8-3) trained with *trainlm* with 95% confidence intervals on unseen data; (c) Predictions of stacked neural network (14-7-12-3) trained with *trainlm* with 95% confidence intervals on unseen data.

model, suggest that the BET surface area and attrition index have little to no effect on predicted reactivity and oxygen release. While, the reactivity with methane showed little effect from increasing Fe contents, the Mn content did appear to negatively affect the reactivity with syngas and CH_4. A marginally positive effect on CH_4 reactivity was noticed from increasing the Fe content, BET surface area and attrition index. Oxygen release was found to increase with an increasing Fe and Mn contents and to a lesser extent with increasing BET surface area and

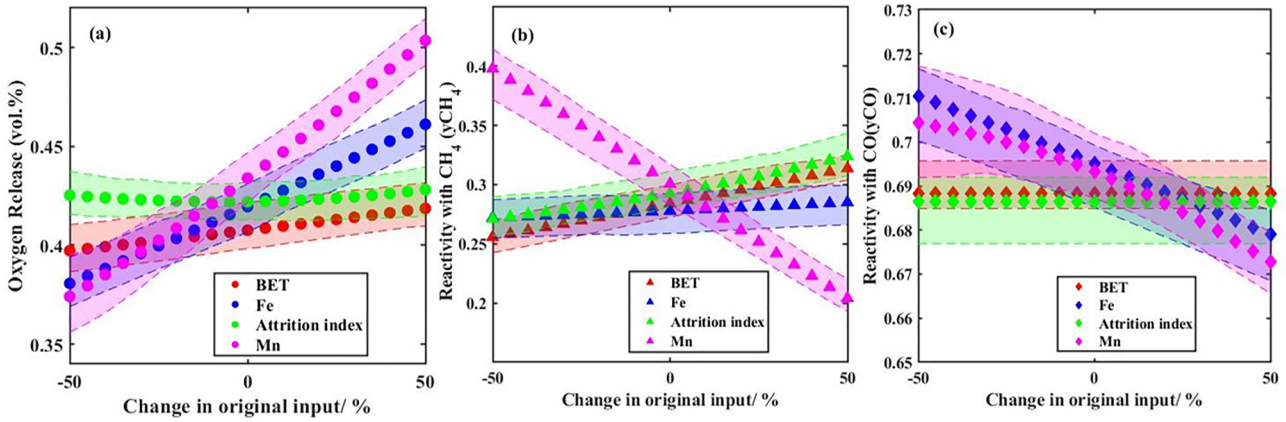

Fig. 5. The predicted performance of reactivity with methane and syngas with 95% confidence intervals with the change in BET surface area, attrition index, and Fe and Mn content of an averaged ore.

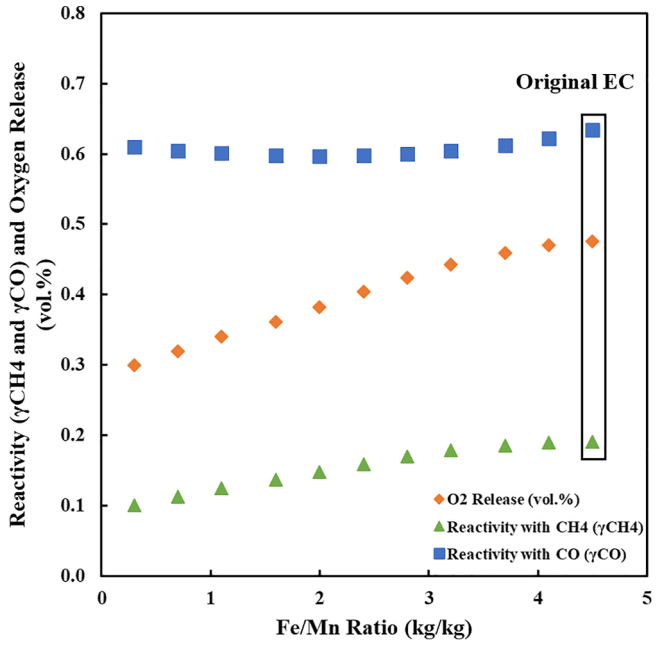

Fig. 6. The predicted effects of varied Fe/Mn mass ratio of manganese ore EC on its oxygen release and reactivity with methane and syngas.

attrition index. This analysis suggests that researchers should focus more on the chemical composition of synthetic oxygen carriers rather than simply aiming for a high surface area or high crushing strength material. Similarly, researchers using natural ores should select materials primarily based on their chemical composition (Fe and Mn content and other minor elemental species) rather than their physical characteristics. However, it should be noted that there is likely a minimum cut-off value for BET surface area and attrition index, below which material are unsuitable for use in chemical-looping reactions.

3.4. Fe/Mn content in manganese ores

In the experimental investigations [22,23], it was observed that the higher the Fe/Mn ratio the greater the oxygen release and methane conversion. Using this knowledge, we can demonstrate the effect of different Fe/Mn mass ratios on the oxygen release and reactivity with different fuels by artificially modifying of the input values of Fe for the EC ore using the trained ANNs. The EC ore has the highest mass concentration of Fe (normalised input 1) and the lowest mass concentration of Mn (normalised input 0) than any other ores investigated in this work and so offers a good starting point ore to vary the Fe/Mn from. The new dataset has been generated by only modifying the normalised input of Fe content of the EC ore from 0 to 1 at 0.1 intervals, and thus different Fe/Mn mass ratios were achieved. The ANN model with the lowest MAE and R^2 determination coefficient has been applied to predict the performance of the new dataset of modified EC ores. Fig. 6 shows oxygen release rate and reactivity with different fuels of modified versions of EC ore where the Fe/Mn ratio was varied from 0.3 to 4.5. The results indicate that both oxygen release rate and reactivity with methane improved with higher ratios of Fe/Mn while the effects on reactivity with syngas are relatively small. This highlights the fact that it may be possible to synthetically increase the Fe/Mn ratio of some manganese ores/oxygen carriers to achieve enhanced performance.

3.5. Discussion

Oxygen carrying materials have been largely investigated experimentally, however there been has limited work on investigation of the oxygen carriers by applying ML algorithms. In this work, it is shown that ANNs can utilised as a prediction tool to estimate the reactivity of different manganese ores with different fuels for chemical-looping.

It is worth noting that artificial neural networks are a data-driven method and the accuracy and robustness of ANNs is largely influenced by the availability of reliable training data and therefore the precision of these predictions is only ever as good as the initial experimental training data. It is generally assumed that a large amount of good experimental data is readily available for oxygen carriers in chemical-looping due to the numerous studies that have been carried out and consequently the extensive number of publications on oxygen carrying materials for the chemical-looping processes. In practice however, it is problematic to collect a large amount of data on oxygen carriers for the chemical-looping processes to establish a training database. The main reason for this is that different experimental apparatuses (such as the thermogravimetric analysers, and fixed- and fluidised- bed reactors) are used, leading to very different results due to intra-particle mass transfer limitations [52], and the same oxygen carriers may exhibit a different performance in different reactors. Also, different researchers may define reactivity of oxygen carriers in different ways; for instance, some researchers evaluate the reactivity of oxygen carriers based on the oxygen carrier conversion, while others use the CO_2 yield to indicate the reactivity of oxygen carriers with different fuels [53]. These reasons made it impractical to combine data from multiple literature sources into a single dataset.

In this work, we have used the experimental data, gathered at Chalmers University of Technology, of different manganese ores from different mines around the world, which cover a broad range of ores, to form the training data for ANNs. It was feasible to implement ANNs to discover the relationships between the input features and the outputs, and the most optimally performing ANNs were able act as predictor to estimate the likely performance of new manganese ores. Although the size of the training database relative to the number of inputs was relatively small, i.e. 171:14, several methods were employed to ensure that the model minimised overfitting and maintained its generality. For instance, 1) the data was normalised and randomly divided into a training dataset, 2) different training algorithms were applied to study the generality of the models, 3) a cross-validation based on the early stopping mechanism was used, and 4) stacked neural networks were adopted to prevent overfitting of the ANNs.

In addition to this, we have compared the results of the ANNs with 14 inputs with reduced-input ANNs where only the most important and highest correlating features were used as inputs. These features were selected based on a Pearson correlation and feature selection analysis. Upon comparison, the results indicated that the reduced-input models did not improve the robustness or accuracy of ANNs. We explain the reason for this is because the physical and chemical properties of manganese ores are complex and reducing the number of input variables of the ANNs will ignore some relatively minor, but important, features relevant to the oxygen carriers' performance. It should be mentioned that ANNs have been successfully applied elsewhere with limited datasets, of similar scale to ours, to predict the performance and properties in materials science [54–56].

Stacked ANNs with bootstrap resampling technology was applied to show the confidence bounds of the model predictions on unseen data and indicated that the selected ANNs have high prediction efficiency for both the new dataset and training dataset. These results indicate that it is feasible to implement ANN or other ML techniques to assist in investigating the reactivity of oxygen-carrying materials and designing new oxygen carriers as illustrated in Fig. 1. ML can potentially spot links in datasets that would otherwise be missed and could lead to new materials being selectively designed and manufactured with desired properties or characteristics. Similar to the predictive sensitive analysis of the selected inputs and the analysis of the impact of Fe/Mn ratio on the performance of manganese ores in chemical-looping processes, other effects such as varied inputs on the predicted results can be estimated. This can potentially provide useful information for

optimisation and synthesis of oxygen-carrying materials.

In this work, an analysis of the different weights for the different inputs (see Fig. 2) rendered complex correlations: the magnitude of the weights of an input throughout the layers (three weights for double-hidden-layers ANNs) can change in comparison to the weights of other inputs. For example, when only comparing the first layer, the weight of the input (e.g., temperature) is larger than that of the other input node weights. However, according to the second layer, the input (e.g., elemental concentration of magnesium) has the highest weighting. This creates complex interlinked connections and as a result the weights change dynamically throughout the layers. Consequently, no general conclusions regarding the importance of the different inputs can be deduced based on the weights and biases produced by the ANN training algorithms. More research is required on producing an explainable ANN for non-classification datasets. We have investigated the potential effect of changing some of the input values on the expected outputs, and it can be seen that the inputs of Fe and Mn have more effects on the predicted data, which is also observed in tests of various manganese ores [22,44].

The ANNs developed in this work were focused on the experimental investigation of manganese ores as oxygen carriers for CLC and CLOU in a batch, lab-scale, fluidised bed reactor. Because of this, these models may have some experimental testing bias and therefore as the results are not based on empirical or intrinsic data, they may not accurately estimate the performance of the same oxygen carrier ore in a different testing facility. Furthermore, the important parameters of oxygen carriers, such as lifetime and long-term performance of oxygen carriers, were not considered in these ANNs but should be investigated in the future. The issue related to prediction accuracy of material properties based on physical-chemical descriptors has also been faced by other applications of ML in chemistry and chemical engineering. For instance, Skoraczyński et al. [57] indicated that the current descriptors are insufficient to predict the outcomes of organic reactions, and the new fundamental chemical descriptors should be developed to improve the performance of ML models. This is also the reason why the predictive sensitive analysis of the inputs shows that chemical compositions (Fe and Mn) of ores have larger impacts than their physical parameters (BET surface area and attrition index). The quantity and quality of the training dataset play a significant role in the performance of the ANN models and what useful information we can extract from the data. The performance data of the manganese ores in a variety of different reactors would be a useful addition to the dataset to aid the development of ANNs that can predict the performance of manganese ores as oxygen carriers for a variety of different applications, for instance, OCAC, CLR, CLG, CLC and CLOU.

4. Summary and conclusions

In this work, we demonstrated an approach to predict the reactivity of manganese ores as oxygen-carrying materials in chemical-looping processes using machine learning (ML) algorithms named artificial neural networks (ANNs). We illustrate and discuss several methods such as different training algorithms, optimal topology and stacked ANNs with bootstrap techniques to prevent the overfitting with small datasets. We showed that trained ANNs can provide very good performance predictions for heterogeneous, multi-component materials (oxygen carrier ores) for chemical-looping processes. These models were tested on unseen experimental and demonstrated their high level of accuracy and generality. The most optimal ANN model for the manganese ores reactivity predictions had a topology of 14-13-3 and was trained with the *trainbr* algorithm, which was able to achieve the highest R^2 (0.94) and lowest MAE (0.057).

ML is an effective approach to estimate the performance of oxygen-carrying materials for the chemical-looping process, and it improved as more datasets of oxygen-carrying materials were generated. These algorithms potentially offer new insights into historical research data on oxygen carriers in chemical-looping processes and could provide a rapid tool to predict the performance of oxygen-carrying materials without the need for significant further experimental investigation and reduce the testing time and cost to evaluate and develop new oxygen-carrier materials. We envisage that ML will accelerate the discovery, design, synthesis, and characterisation of oxygen-carrier materials for chemical-looping processes.

Declaration of Competing Interest

The authors declare that they have no known competing financial interests or personal relationships that could have appeared to influence the work reported in this paper.

Acknowledgments

PTC and EJA would like to thank the EPSRC and UKCCSRC for financial support through grant EP/P026214/1. YYL would like to acknowledge the financial support from the Cranfield University Energy and Power research bursary and Erasmus + scheme. TM and YYL would like to thank the support from Chalmers Energy Area of Advances. Data from this research can be accessed through Cranfield University's data storage and recovery site - Cranfield Online Research Data (CORD) - https://figshare.com/s/0fe1f7a5c4269c8dc373.

Appendix A. Supplementary data

Supplementary data to this article can be found online at https://doi.org/10.1016/j.cej.2020.124072.

References

[1] T. Mattisson, A. Lyngfelt, H. Leion, Chemical-looping with oxygen uncoupling for combustion of solid fuels, Int. J. Greenh. Gas Control. 3 (2009) 11–19, https://doi.org/10.1016/J.IJGGC.2008.06.002.
[2] A. Lyngfelt, B. Leckner, T. Mattisson, A fluidized-bed combustion process with inherent CO_2 separation; application of chemical-looping combustion, Chem. Eng. Sci. 56 (2001) 3101–3113, https://doi.org/10.1016/S0009-2509(01)00007-0.
[3] J. Adanez, A. Abad, F. Garcia-Labiano, P. Gayan, L.F. de Diego, Progress in chemical-looping combustion and reforming technologies, Prog. Energy Combust. Sci. 38 (2012) 215–282, https://doi.org/10.1016/J.PECS.2011.09.001.
[4] M. Rydén, A. Lyngfelt, Using steam reforming to produce hydrogen with carbon dioxide capture by chemical-looping combustion, Int. J. Hydrogen Energy. 31 (2006) 1271–1283, https://doi.org/10.1016/J.IJHYDENE.2005.12.003.
[5] T. Mattisson, A. Lyngfelt, Applications of chemical-looping combustion with capture of CO_2, Control. (2001) 46–51. http://www.entek.chalmers.se/anly/symp/symp2001.html (accessed June 14, 2019).
[6] L.-S. Fan, Chemical Looping Partial Oxidation: Gasification, Reforming, and Chemical Syntheses, 2017. DOI: 10.1017/9781108157841.
[7] Q. Guo, Y. Cheng, Y. Liu, W. Jia, H.J. Ryu, Coal chemical looping gasification for syngas generation using an iron-based oxygen carrier, Ind. Eng. Chem. Res. 53 (2014) 78–86, https://doi.org/10.1021/ie401568x.
[8] M. Rydén, M. Hanning, A. Corcoran, F. Lind, Oxygen Carrier Aided Combustion (OCAC) of wood chips in a semi-commercial circulating fluidized bed boiler using manganese ore as bed material, Appl. Sci. 6 (2016) 347, https://doi.org/10.3390/app6110347.
[9] H. Thunman, F. Lind, C. Breitholtz, N. Berguerand, M. Seemann, Using an oxygen-carrier as bed material for combustion of biomass in a 12-MWth circulating fluidized-bed boiler, Fuel 113 (2013) 300–309, https://doi.org/10.1016/j.fuel.2013.05.073.
[10] Q. Imtiaz, D. Hosseini, C.R. Müller, Review of oxygen carriers for chemical looping with oxygen uncoupling (CLOU): thermodynamics material development, and synthesis, Energy Technol. 1 (2013) 633–647, https://doi.org/10.1002/ente.201300099.
[11] J.C. Abanades, B. Arias, A. Lyngfelt, T. Mattisson, D.E. Wiley, H. Li, M.T. Ho, E. Mangano, S. Brandani, Emerging CO_2 capture systems, Int. J. Greenh. Gas Control. 40 (2015) 126–166, https://doi.org/10.1016/j.ijggc.2015.04.018.
[12] M. Bui, C.S. Adjiman, A. Bardow, E.J. Anthony, A. Boston, S. Brown, P.S. Fennell, S. Fuss, A. Galindo, L.A. Hackett, J.P. Hallett, H.J. Herzog, G. Jackson, J. Kemper, S. Krevor, G.C. Maitland, M. Matuszewski, I.S. Metcalfe, C. Petit, G. Puxty, J. Reimer, D.M. Reiner, E.S. Rubin, S.A. Scott, N. Shah, B. Smit, J.P.M. Trusler, P. Webley, J. Wilcox, N. Mac Dowell, Carbon capture and storage (CCS): the way forward, Energy Environ. Sci. 11 (2018) 1062–1176, https://doi.org/10.1039/c7ee02342a.
[13] A. Lyngfelt, A. Brink, Ø. Langørgen, T. Mattisson, M. Rydén, C. Linderholm, 11,000 h of chemical-looping combustion operation—where are we and where do we want to go? Int. J. Greenh. Gas Control. 88 (2019) 38–56, https://doi.org/10.1016/J.

IJGGC.2019.05.023.
[14] P. Fennell, B. Anthony. Calcium and chemical looping technology for power generation and carbon dioxide (CO_2) capture, 2015.
[15] A. Fossdal, E. Bakken, B.A. Øye, C. Schøning, I. Kaus, T. Mokkelbost, Y. Larring, Study of inexpensive oxygen carriers for chemical looping combustion, Int. J. Greenh. Gas Control. 5 (2011) 483–488, https://doi.org/10.1016/j.ijggc.2010.08.001.
[16] A. Lyngfelt, Oxygen carriers for chemical looping combustion - 4000 h of operational experience, Oil Gas Sci. Technol. 66 (2011) 161–172, https://doi.org/10.2516/ogst/2010038.
[17] M.M. Hossain, H.I. de Lasa, Chemical-looping combustion (CLC) for inherent CO_2 separations—a review, Chem. Eng. Sci. 63 (2008) 4433–4451, https://doi.org/10.1016/J.CES.2008.05.028.
[18] T. Mattisson, Materials for chemical-looping with oxygen uncoupling, ISRN Chem. Eng. 2013 (2013) 1–19, https://doi.org/10.1155/2013/526375.
[19] H. Leion, T. Mattisson, A. Lyngfelt, Use of ores and industrial products as oxygen carriers in chemical-looping combustion, Energy Fuels 23 (2009) 2307–2315, https://doi.org/10.1021/ef8008629.
[20] H. Leion, A. Lyngfelt, M. Johansson, E. Jerndal, T. Mattisson, The use of ilmenite as an oxygen carrier in chemical-looping combustion, Chem. Eng. Res. Des. 86 (2008) 1017–1026, https://doi.org/10.1016/j.cherd.2008.03.019.
[21] M. Arjmand, H. Leion, T. Mattisson, A. Lyngfelt, Investigation of different manganese ores as oxygen carriers in chemical-looping combustion (CLC) for solid fuels, Appl. Energy 113 (2014) 1883–1894, https://doi.org/10.1016/j.apenergy.2013.06.015.
[22] S. Sundqvist, M. Arjmand, T. Mattisson, M. Rydén, A. Lyngfelt, Screening of different manganese ores for chemical-looping combustion (CLC) and chemical-looping with oxygen uncoupling (CLOU), Int. J. Greenh. Gas Control. 43 (2015) 179–188, https://doi.org/10.1016/j.ijggc.2015.10.027.
[23] S. Sundqvist, N. Khalilian, H. Leion, T. Mattisson, A. Lyngfelt, Manganese ores as oxygen carriers for chemical-looping combustion (CLC) and chemical-looping with oxygen uncoupling (CLOU), J. Environ. Chem. Eng. 5 (2017) 2552–2563, https://doi.org/10.1016/j.jece.2017.05.007.
[24] C. Linderholm, M. Schmitz, M. Biermann, M. Hanning, A. Lyngfelt, Chemical-looping combustion of solid fuel in a 100 kW unit using sintered manganese ore as oxygen carrier, Int. J. Greenh. Gas Control. 65 (2017) 170–181, https://doi.org/10.1016/J.IJGGC.2017.07.017.
[25] M. Schmitz, C. Linderholm, P. Hallberg, S. Sundqvist, A. Lyngfelt, Chemical-looping combustion of solid fuels using manganese ores as oxygen carriers, Energy Fuels 30 (2016) 1204–1216, https://doi.org/10.1021/acs.energyfuels.5b02440.
[26] P. Moldenhauer, M. Rydén, T. Mattisson, M. Younes, A. Lyngfelt, The use of ilmenite as oxygen carrier with kerosene in a 300 W CLC laboratory reactor with continuous circulation, Appl. Energy 113 (2014) 1846–1854, https://doi.org/10.1016/J.APENERGY.2013.06.009.
[27] P. Moldenhauer, M. Rydén, A. Lyngfelt, Testing of minerals and industrial by-products as oxygen carriers for chemical-looping combustion in a circulating fluidized-bed 300 W laboratory reactor, Fuel 93 (2012) 351–363, https://doi.org/10.1016/j.fuel.2011.11.009.
[28] H. Leion, E. Jerndal, B.M. Steenari, S. Hermansson, M. Israelsson, E. Jansson, M. Johnsson, R. Thunberg, A. Vadenbo, T. Mattisson, A. Lyngfelt, Solid fuels in chemical-looping combustion using oxide scale and unprocessed iron ore as oxygen carriers, Fuel 88 (2009) 1945–1954, https://doi.org/10.1016/j.fuel.2009.03.033.
[29] T. Song, J. Wu, H. Zhang, L. Shen, Characterization of an Australia hematite oxygen carrier in chemical looping combustion with coal, Int. J. Greenh. Gas Control. 11 (2012) 326–336, https://doi.org/10.1016/j.ijggc.2012.08.013.
[30] L. Shen, J. Wu, J. Xiao, Q. Song, R. Xiao, Chemical-looping combustion of biomass in a 10 kWth reactor with iron oxide as an oxygen carrier, Energy Fuels 23 (2009) 2498–2505, https://doi.org/10.1021/ef900033n.
[31] A. Cuadrat, A. Abad, F. García-Labiano, P. Gayán, L.F. de Diego, J. Adánez, The use of ilmenite as oxygen-carrier in a 500Wth Chemical-Looping Coal Combustion unit, Int. J. Greenh. Gas Control. 5 (2011) 1630–1642, https://doi.org/10.1016/j.ijggc.2011.09.010.
[32] J. Mohd Ali, M.A. Hussain, M.O. Tade, J. Zhang, Artificial Intelligence techniques applied as estimator in chemical process systems – a literature survey, Expert Syst. Appl. 42 (2015) 5915–5931, https://doi.org/10.1016/j.eswa.2015.03.023.
[33] J. Panteleev, H. Gao, L. Jia, Recent applications of machine learning in medicinal chemistry, Bioorgan. Med. Chem. Lett. 28 (2018) 2807–2815, https://doi.org/10.1016/j.bmcl.2018.06.046.
[34] S. Kalogirou, Applications of artificial neural networks in energy systems, Energy Convers. Manage. 40 (1999) 1073–1087, https://doi.org/10.1016/S0196-8904(99)00012-6.
[35] M.A. Duchesne, A. MacChi, D.Y. Lu, R.W. Hughes, D. McCalden, E.J. Anthony, Artificial neural network model to predict slag viscosity over a broad range of temperatures and slag compositions, Fuel Process. Technol. Elsevier, 2010, pp. 831–836, , https://doi.org/10.1016/j.fuproc.2009.10.013.
[36] S.A. Kalogirou, Artificial neural networks in renewable energy systems applications: a review, Renew. Sustain. Energy Rev. 5 (2001) 373–401, https://doi.org/10.1016/S1364-0321(01)00006-5.
[37] B.R. Hough, D.A.C. Beck, D.T. Schwartz, J. Pfaendtner, Application of machine learning to pyrolysis reaction networks: reducing model solution time to enable process optimization, Comput. Chem. Eng. 104 (2017) 56–63, https://doi.org/10.1016/j.compchemeng.2017.04.012.
[38] N. Sipöcz, F.A. Tobiesen, M. Assadi, The use of Artificial Neural Network models for CO_2 capture plants, Appl. Energy 88 (2011) 2368–2376, https://doi.org/10.1016/J.APENERGY.2011.01.013.
[39] Q. Zhou, Y. Wu, C.W. Chan, P. Tontiwachwuthikul, Modeling of the carbon dioxide capture process system using machine intelligence approaches, Eng. Appl. Artif. Intell. 24 (2011) 673–685, https://doi.org/10.1016/j.engappai.2011.01.003.
[40] K. Fu, G. Chen, T. Sema, X. Zhang, Z. Liang, R. Idem, P. Tontiwachwuthikul, Experimental study on mass transfer and prediction using artificial neural network for CO_2 absorption into aqueous, DETA (2013), https://doi.org/10.1016/j.ces.2013.04.024.
[41] F. Li, J. Zhang, E. Oko, M. Wang, Modelling of a post-combustion CO_2 capture process using neural networks, Fuel 151 (2015) 156–163, https://doi.org/10.1016/j.fuel.2015.02.038.
[42] M.T. Dunstan, A. Jain, W. Liu, S.P. Ong, T. Liu, J. Lee, K.A. Persson, S.A. Scott, J.S. Dennis, C.P. Grey, Large scale computational screening and experimental discovery of novel materials for high temperature CO_2 capture, Energy Environ. Sci. 9 (2016) 1346–1360, https://doi.org/10.1039/c5ee03253a.
[43] C.Y. Lau, M.T. Dunstan, W. Hu, C.P. Grey, S.A. Scott, Large scale in silico screening of materials for carbon capture through chemical looping, Energy Environ. Sci. 10 (2017) 818–831, https://doi.org/10.1039/c6ee02763f.
[44] S. Sundqvist, Chalmers tekniska högskola. Department of Chemistry and Chemical Engineering, Manganese ores as oxygen carriers for chemical-looping combustion, Chalmers University of Technology, 2017. https://research.chalmers.se/en/publication/251617 (accessed September 2, 2019).
[45] K.T. Butler, D.W. Davies, H. Cartwright, O. Isayev, A. Walsh, Machine learning for molecular and materials science, Nature 559 (2018) 547–555, https://doi.org/10.1038/s41586-018-0337-2.
[46] M. Asadi-Eydivand, M. Solati-Hashjin, A. Farzadi, N.A.A. Osman, Artificial neural network approach to estimate the composition of chemically synthesized biphasic calcium phosphate powders, Ceram. Int. 40 (2014) 12439–12448, https://doi.org/10.1016/j.ceramint.2014.04.095.
[47] J. Zhang, E.B. Martin', A.J. Morris, C. Kiparissides, Inferential Estimation of Polymer Quality Using Stacked Neural Networks, 1997. https://pdf.sciencedirectassets.com/271414/1-s2.0-S0098135400X02062/1-s2.0-S0098135497876375/main.pdf?x-amz-security-token=AgoJb3JpZ2luX2VjEHIaCXVzLWVhc3QtMSJHMEUCIQDTZtderEH6rMv9yg352KykuMH0ZSbMJbsC6n%2Fzv7fYwgIgcBA5yrpXIvFgXALG1uVB2El3zzYiEaZZ7ktS011vSS (accessed March 28, 2019).
[48] S.J. Joyce, D.J. Osguthorpe, J.A. Padgett, G.J. Price, Neural network prediction of glass-transition temperatures from monomer structure, J. Chem. Soc. Faraday Trans. 91 (1995) 2491–2496, https://doi.org/10.1039/FT9959102491.
[49] H. Yang, Z. Zhang, J. Zhang, X.C. Zeng, Machine learning and artificial neural network prediction of interfacial thermal resistance between graphene and hexagonal boron nitride, Nanoscale 10 (2018) 19092–19099, https://doi.org/10.1039/c8nr05703f.
[50] W. Sha, K.L. Edwards, The use of artificial neural networks in materials science based research, Mater. Des. 28 (2007) 1747–1752, https://doi.org/10.1016/j.matdes.2007.02.009.
[51] A.M. Hassan, A. Alrashdan, M.T. Hayajneh, A.T. Mayyas, Prediction of density, porosity and hardness in aluminum-copper-based composite materials using artificial neural network, J. Mater. Process. Technol. 209 (2009) 894–899, https://doi.org/10.1016/j.jmatprotec.2008.02.066.
[52] Z. Zhang, J.G. Yao, M.E. Boot-Handford, P.S. Fennell, Pressurised chemical-looping combustion of an iron-based oxygen carrier: reduction kinetic measurements and modelling, Fuel Process. Technol. 171 (2018) 205–214, https://doi.org/10.1016/j.fuproc.2017.11.018.
[53] D. Mei, T. Mendiara, A. Abad, L.F. De Diego, F. García-Labiano, P. Gayán, J. Adánez, H. Zhao, Manganese minerals as oxygen carriers for chemical looping combustion of coal, Ind. Eng. Chem. Res. 55 (2016) 6539–6546, https://doi.org/10.1021/acs.iecr.6b00263.
[54] Y. Zhang, C. Ling, A strategy to apply machine learning to small datasets in materials science, Npj Comput. Mater. 4 (2018) 25, https://doi.org/10.1038/s41524-018-0081-z.
[55] S. Feng, H. Zhou, H. Dong, Using deep neural network with small dataset to predict material defects, Mater. Des. 162 (2019) 300–310, https://doi.org/10.1016/j.matdes.2018.11.060.
[56] A. Pasini, Artificial neural networks for small dataset analysis, J. Thorac. Dis. 7 (2015) 953–960, https://doi.org/10.3978/j.issn.2072-1439.2015.04.61.
[57] G. Skoraczyński, P. Dittwald, B. Miasojedow, S. Szymkuć, E.P. Gajewska, B.A. Grzybowski, A. Gambin, Predicting the outcomes of organic reactions via machine learning: are current descriptors sufficient? Sci. Rep. 7 (2017) 3582, , https://doi.org/10.1038/s41598-017-02303-0.